Maximum Power Point Tracking Techniques for Efficient Photovoltaic Microsatellite Power Supply System

Hadi Malek, Sara Dadras, YangQuan Chen
ECE Dept. of Utah State University, Logan, Utah;
Hadi.malek@ieee.org

Robert Burt, James Cook
Space Dynamics Laboratory
1695 N. Research Parkway, North Logan, Utah; 435-713-3337
Robert.Burt@sdl.usu.edu

Outline of Presentation

- Why MPPT?
- Different algorithms
- Extremum Seeking Control
- Hardware Implementation
- Fractional Order Extremum Seeking Control

Maximum power point

- There is an exponential relationship between current and voltage in PV cell.

$$I = I_{SC} - I_{o1}(e^{qV/kT} - 1) - I_{o2}(e^{qV/2kT} - 1)$$

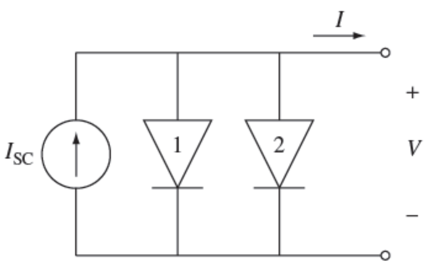

$$I = I'_{SC} - I_{o1}(e^{q(V+IR_S)/kT} - 1) - I_{o2}(e^{q(V+IR_S)/2kT} - 1) - \frac{(V + IR_S)}{R_{Sh}}$$

$$I = I'_{SC} - I_o(e^{q(V+IR_S)/A_o kT} - 1) - \frac{(V + IR_S)}{R_{Sh}}$$

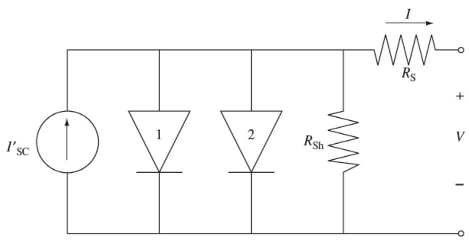

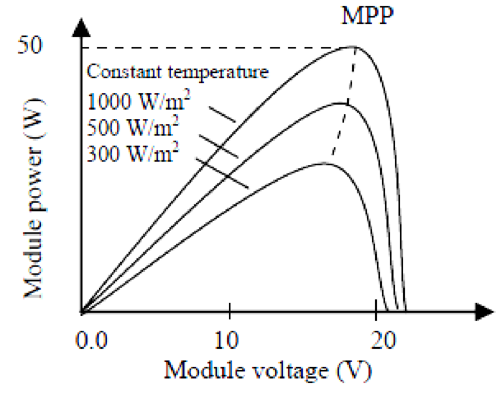

(a)

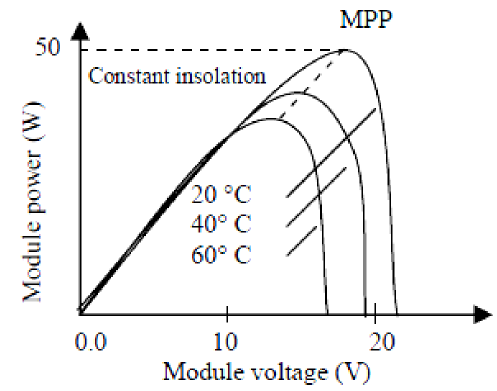

(b)

F. Adamo, F. Attivissimo, M. Spadavecchia, "**A Tool for Photovoltaic Panels Modeling and Testing**", IEEE, 2010

Different Algorithms of MPPT

- Voltage Based Peak Power Tracking.
- Current Based Peak Power Tracking.
- Incremental conductance.
- Perturb & Observe. (P&O)

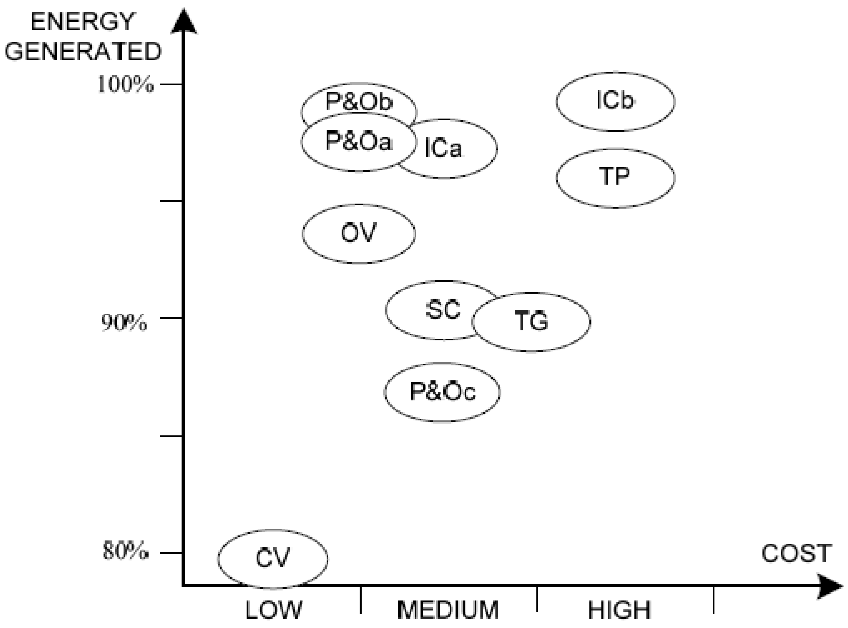

ROBERTO FARANDA, SONIA LEVA, " **Energy comparison of MPPT techniques for PV Systems** " , WSEAS TRANSACTIONS on POWER SYSTEMS, Issue 6, Volume 3, June 2008

Different Algorithms

Perturb and Observation

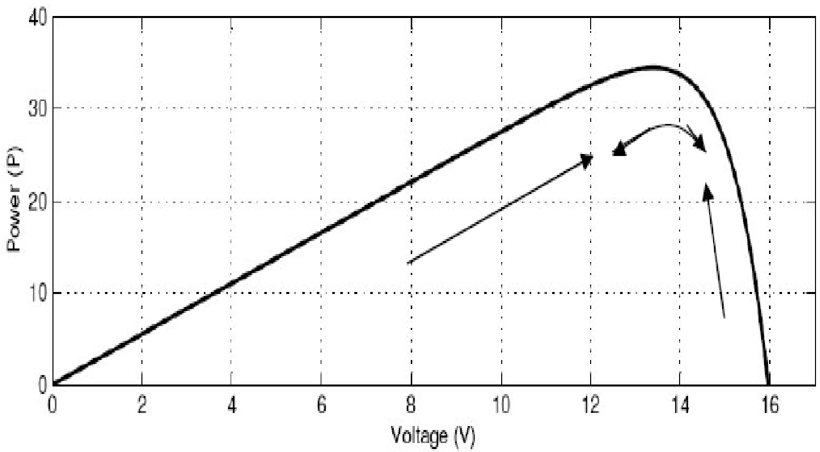

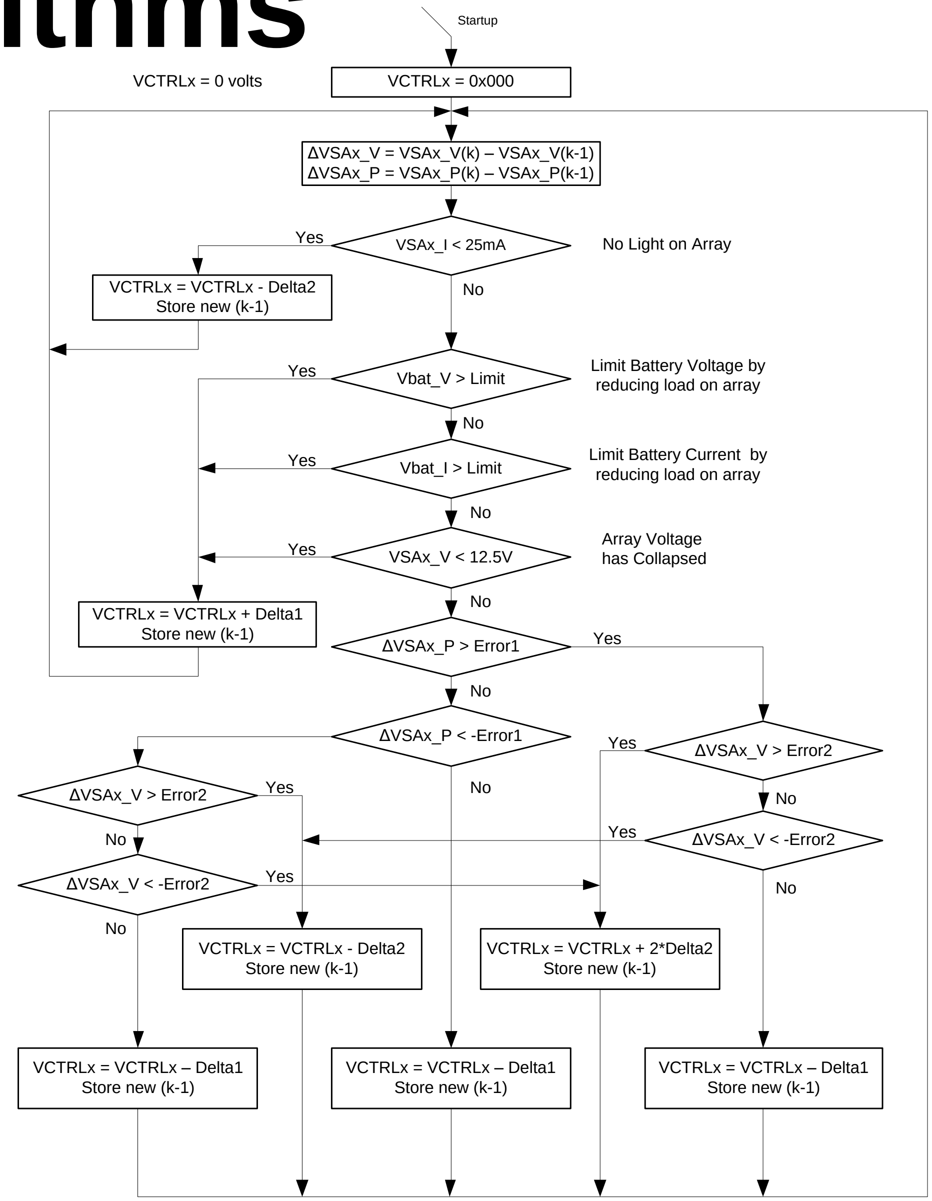

Extremum Seeking Control

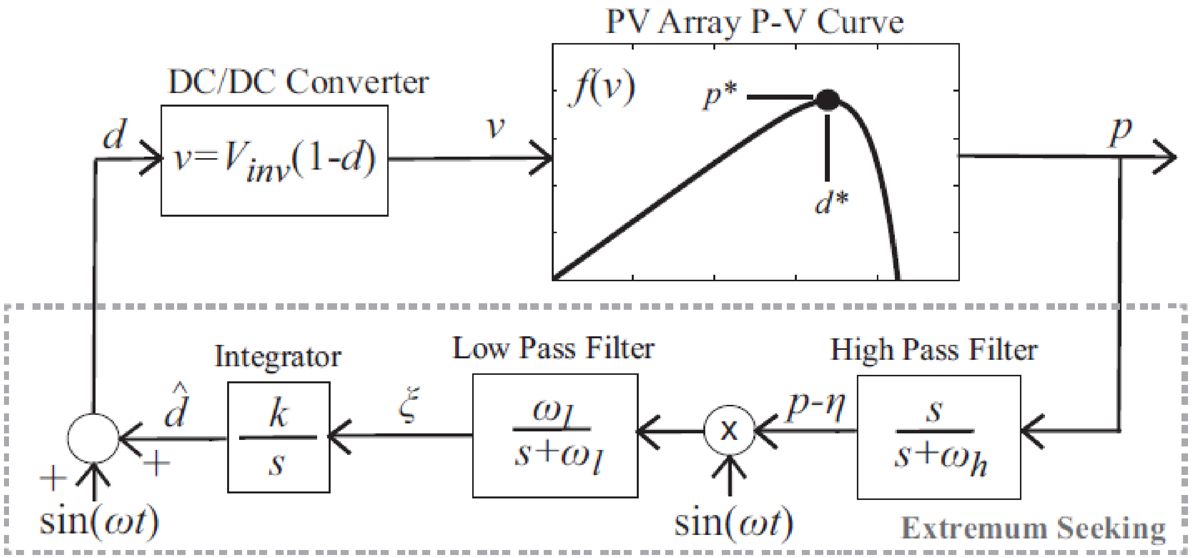

It is crucial to note that all of the plant components are allowed to be unknown.

Extremum Seeking Control

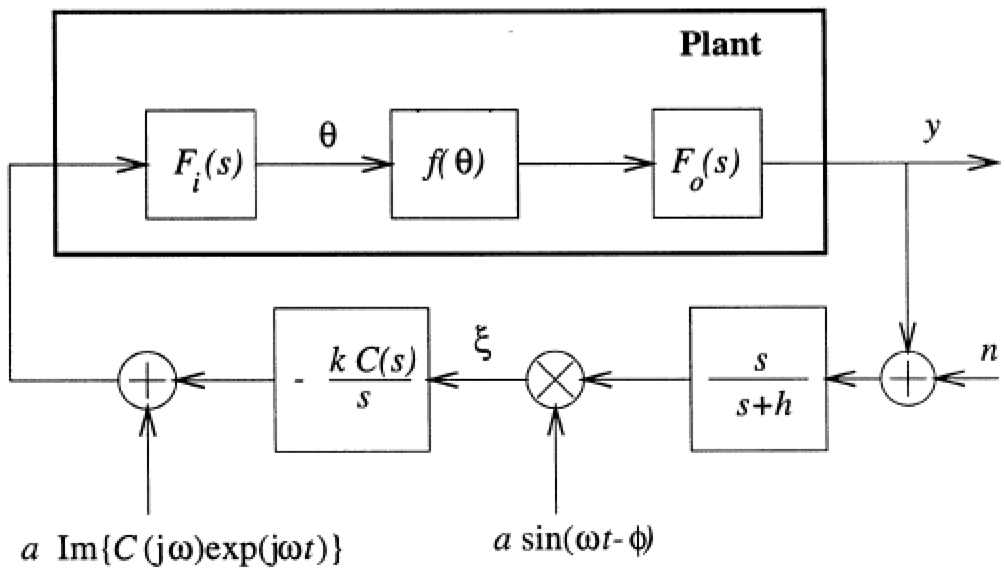

The periodic perturbations used in the loop perform modulation and demodulation, and their role is to make the extremum of the equilibrium map, which is flat, and therefore appears as a zero gain block, appear, in a time-average sense, as a gain proportional to the second derivative at the extremum

The role of the washout filter is to eliminate the bias to the DC component of the equilibrium map

Hardware Implementation

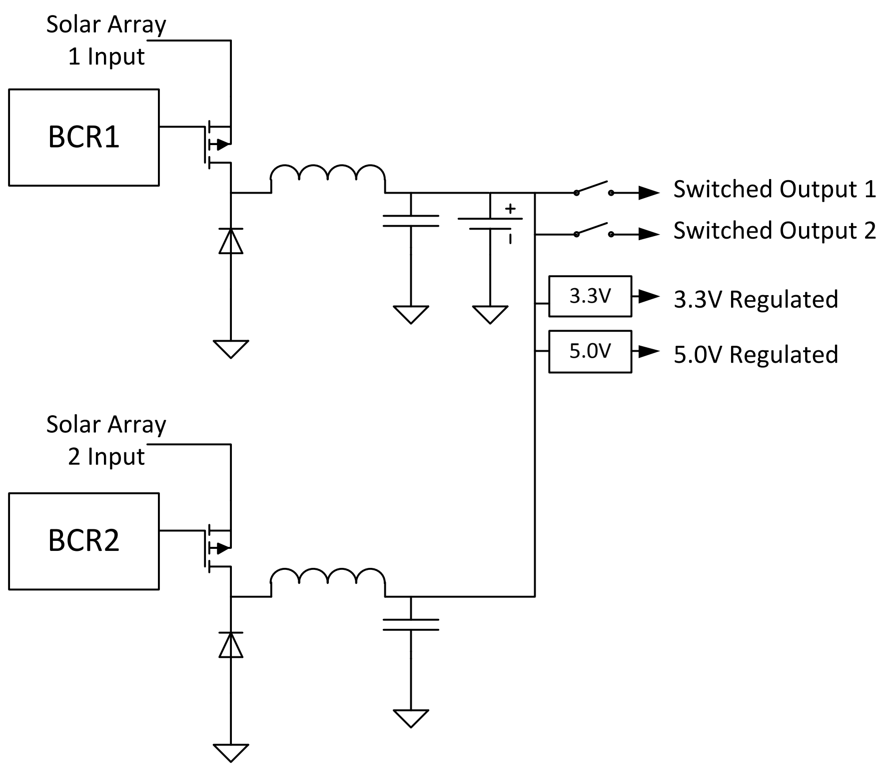

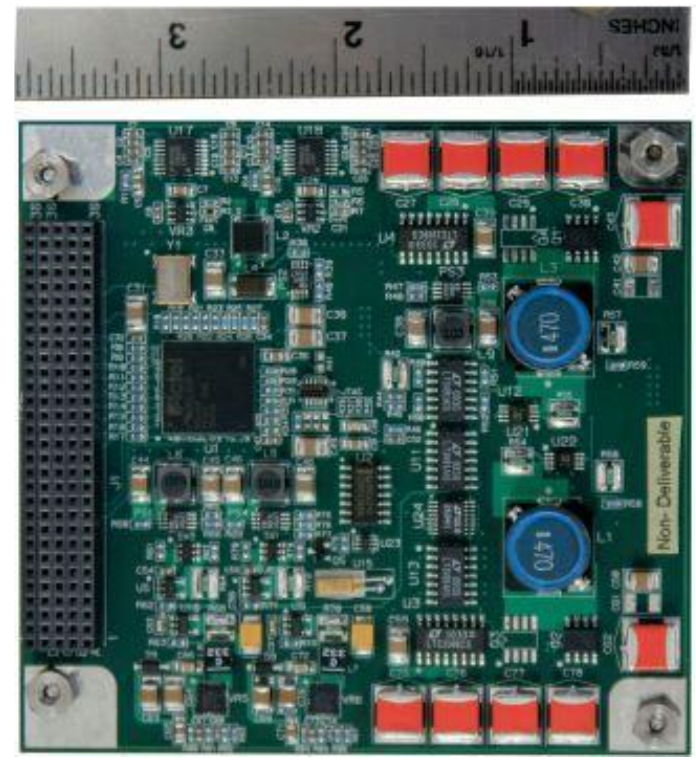

•The EPS includes two solar array inputs that feed into separate Battery Charge Regulators (BCR). The BCRs use a buck converter topology implemented with a current mode DC-DC converter.

Constraints

- An ultra-low power FPGA is used to implement the algorithm and controller. The low power FPGA is a key component. It allows for minimum power consumption by the EPS and was selected due to a higher tolerance to radiation effects over other commercially available components.
- The low power simple architecture forces all algorithms to only use fixed point integer based math, No floating point. This becomes one of the major design constraints for this project.

Experiment Setup

MPPT Test Setup

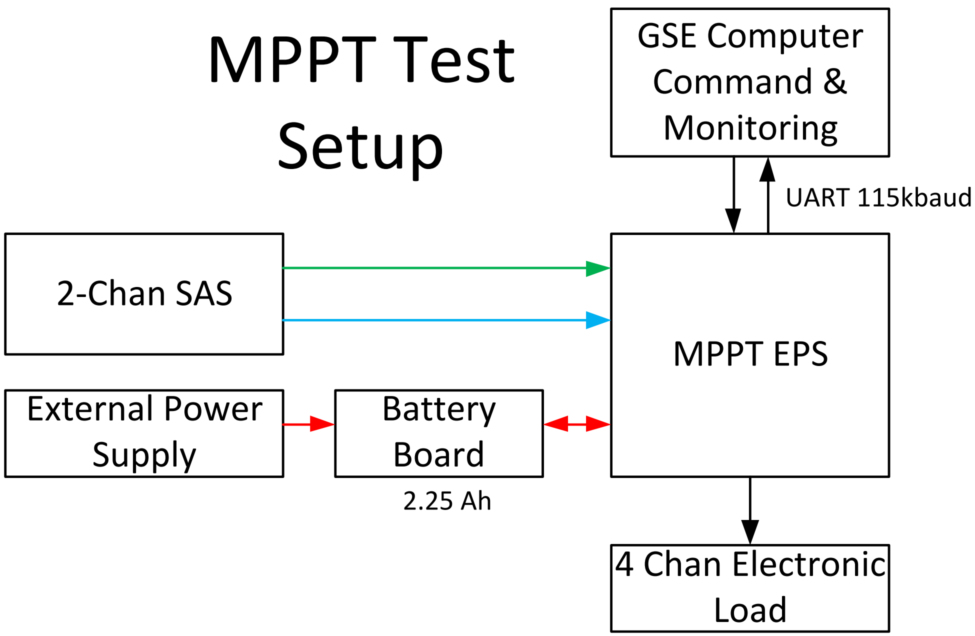

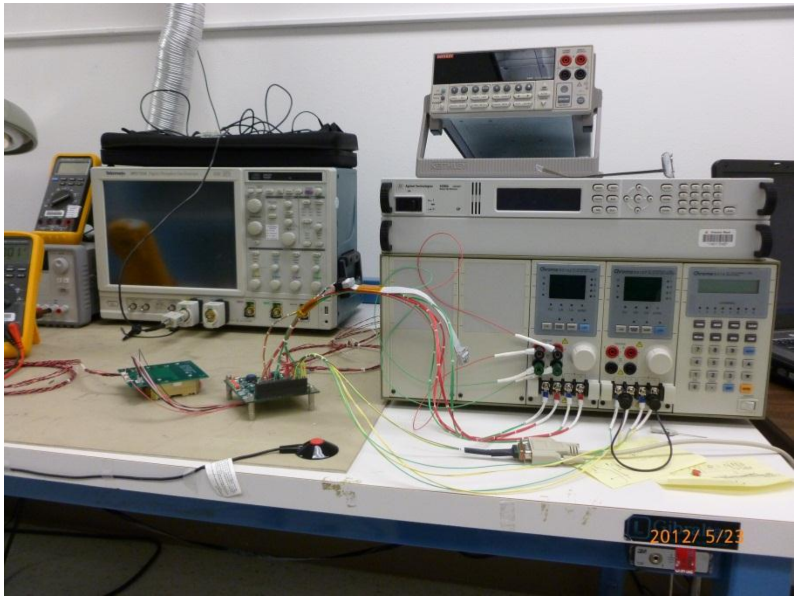

Manufacture	Model Number	Description
Agilent	E3631	Triple Output Power Supply
Agilent	E4360A	Modular SAS Mainframe
Agilent	E4362	Solar Array Simulator Module
Agilent	E4362	Solar Array Simulator Module
Chroma	6314	Electronic Load Mainframe
Chroma	63102	Dual Channel Load Module
Chroma	63107	Dual Channel Load Module
Dell	M90	Laptop Computer + Monitor

Experimental Results

Steady State: This test was a 30 second sample in time of the EPS power output with a fixed solar array input.

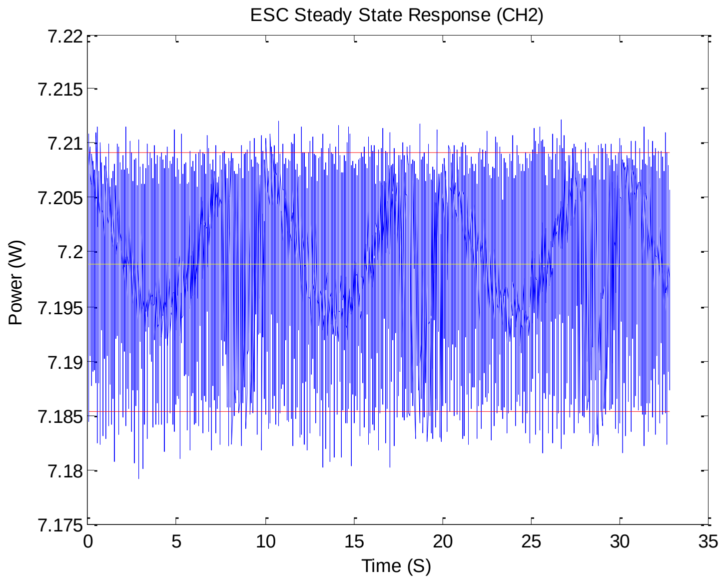

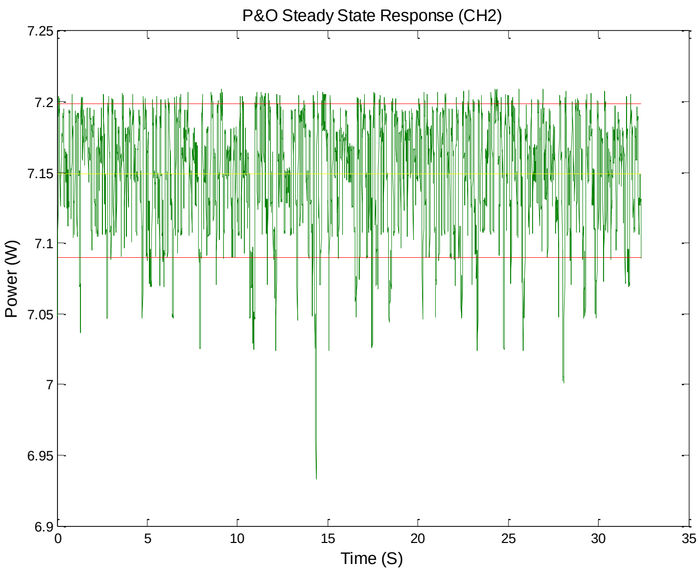

Metric	**ESC Value**	**P&O Value**
Average Peak-to-Peak	0.024 watts	0.109 watts
Average Power	7.199 watts	7.149 watts
Minimum Power Output	7.179 watts	6.933 watts
Maximum Power Output	7.212 watts	7.2093 watts

Experimental Results

Dynamic Testing:

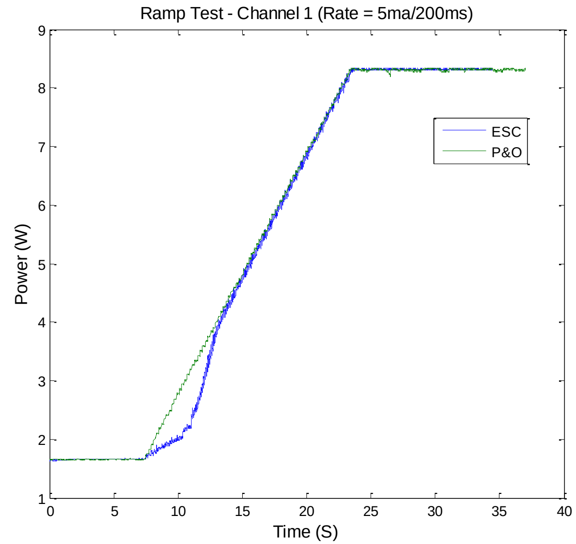

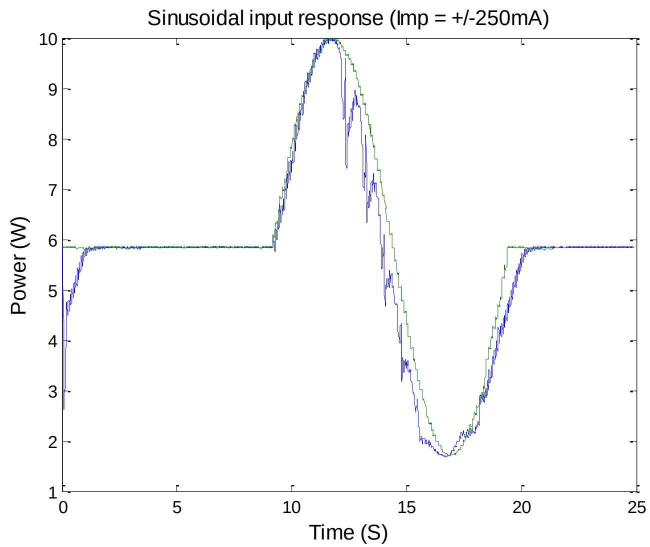

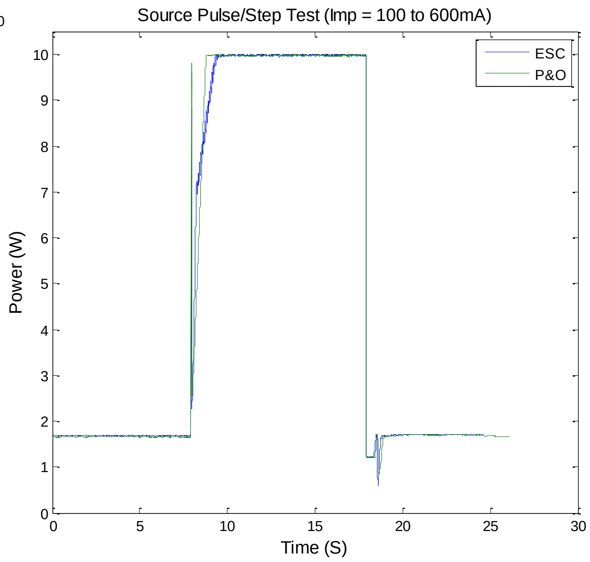

Conclusions:

- ***in the steady state condition, ESC can extract more power from PV panels, has smaller peak-peak power ripple, and provides greater immunity for channel to channel interference in comparison with P&O controller.***

- ***In the dynamic response test, the P&O algorithm clearly outperforms the IO-ESC algorithm as presently implemented.***

- ***Because of time constraints, we were not able to implement the slope seeking control portion of the ESC algorithm and compare it to the P&O. Obviously; ESC cannot follow fast slopes and cannot satisfy high dynamic response MPPT requirements without this slope seeking portion as we can see in the experimental results.***

Fractional Order ESC

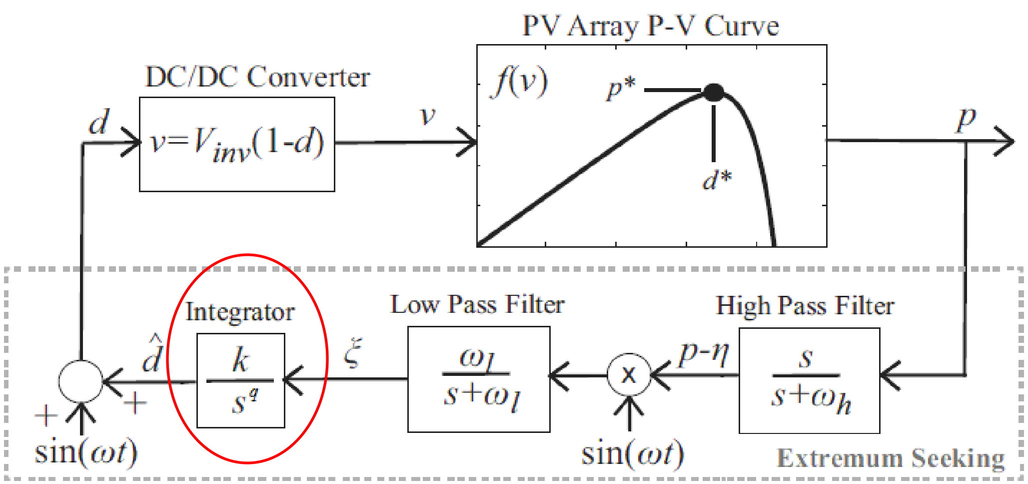

- Replace Integer Order Integrator with Fractional Order Integrator.

Simulation results of FO ESC

without noise | in presence of noise | different integration orders

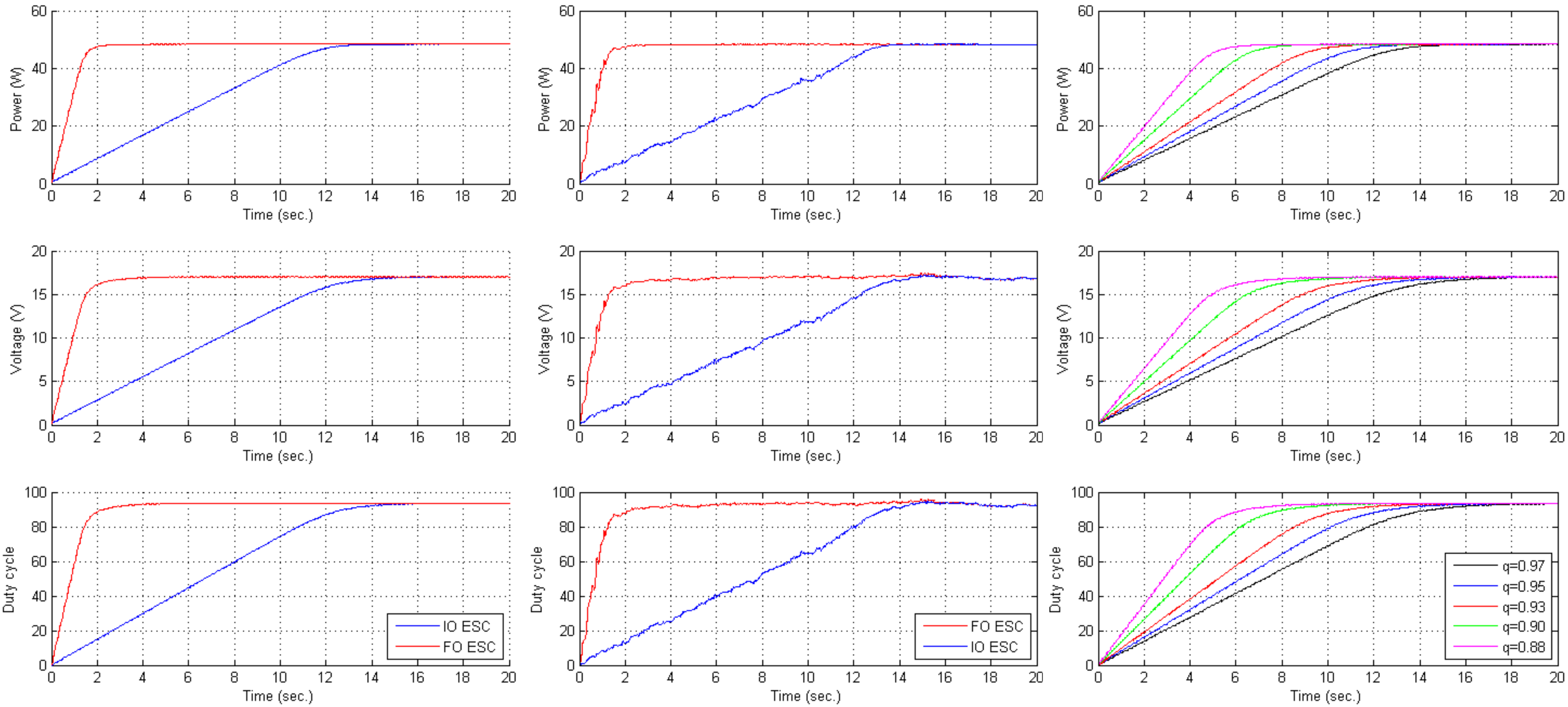

Experimental results of FO ESC

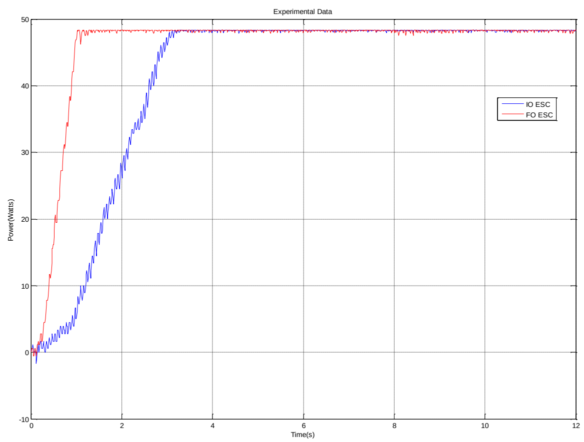

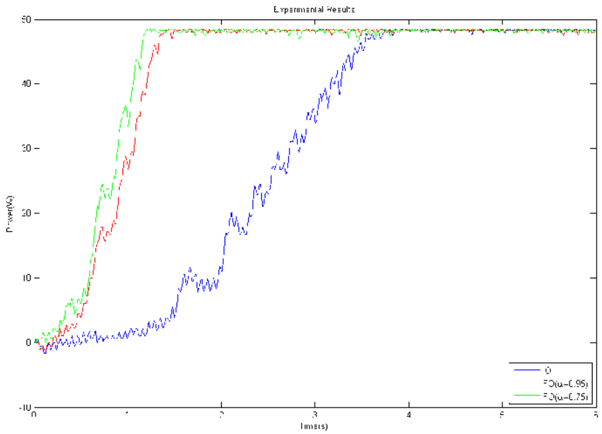

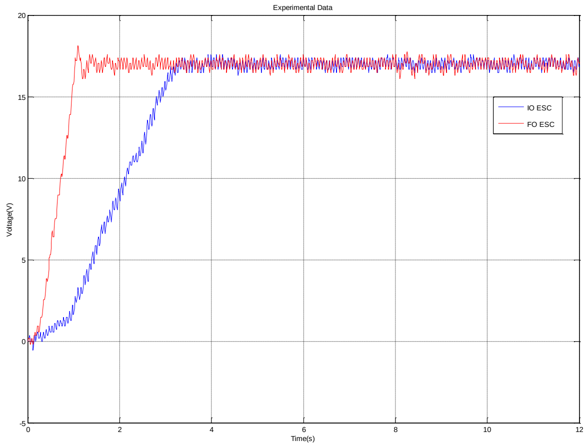

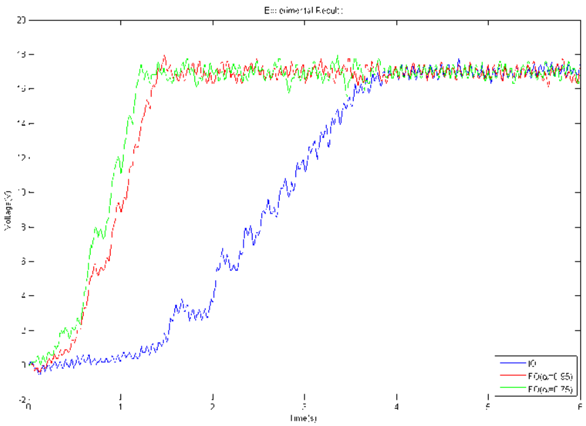

Conclusions:

- ***the fractional order ESC has a better performance in comparison with integer order ESC***.

Acknowledgments

We would like to acknowledge and thank

- The **Air Force Research Laboratory** for providing the funding for this research effort without which it could not have been possible.
- The **Space Dynamics Laboratory** and **Utah State University** for support of time and other laboratory resources involved in the testing.

Thank you!

Q&A?

Space Dynamics LABORATORY
Utah State University Research Foundation

UtahStateUniversity

Extremum Seeking Control

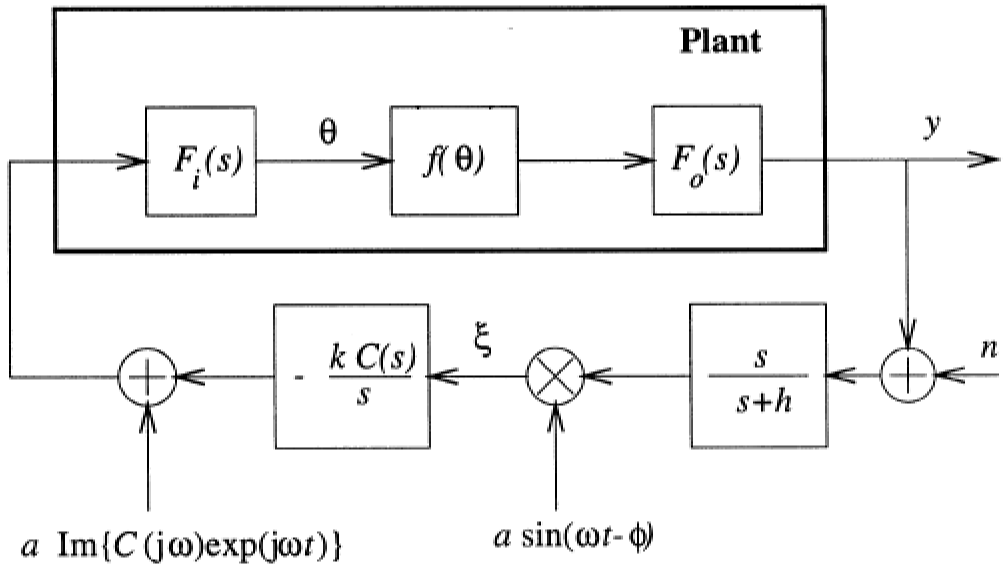

C(s) will be used to improve the stability properties of the extremum seeking scheme.

This compensator can be regarded as a phase-lead compensator which improves the phase margin in a loop with a high relative degree.

One limitation to the speed of adaptation will be imposed by the presence of the measurement noise input n.

Extremum Seeking Control

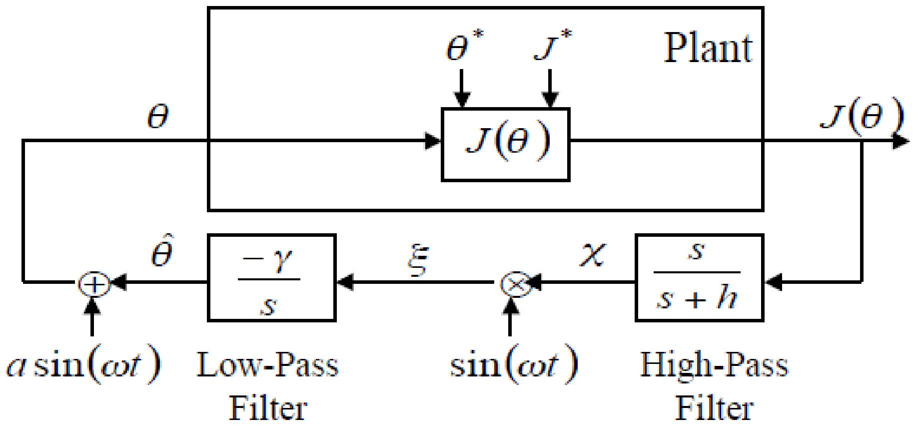

suppose

$$\tilde{\theta} = \theta^* - \hat{\theta}$$

then, based on the above diagram, we have

$$\theta(t) = \hat{\theta}(t) + a\sin(\omega t) \rightarrow \theta(t) = \theta^* - \tilde{\theta} + a\sin(\omega t)$$

$$\rightarrow \theta(t) - \theta^* = -\tilde{\theta} + a\sin(\omega t)$$

Extremum Seeking Control

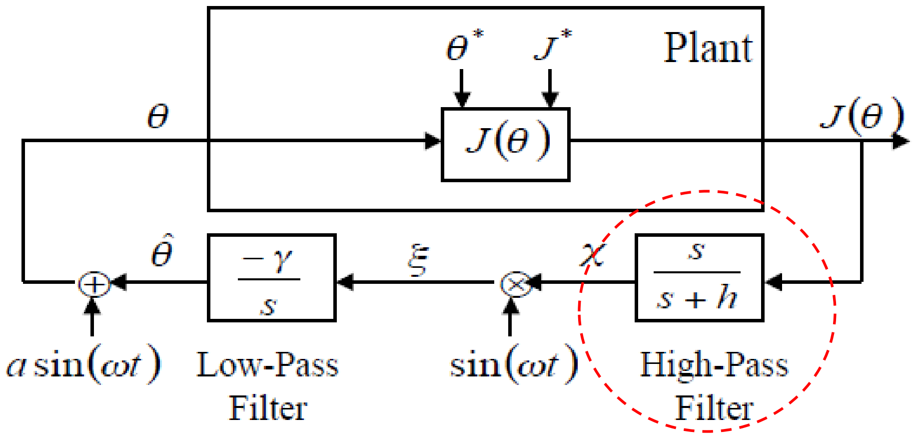

$$J(\theta) = J^* + \frac{J''}{2}(\theta - \theta^*)^2 = J^* + \frac{J''}{2}(a\sin(\omega t) - \tilde{\theta})^2$$

$$= J^* + \frac{J''}{2}a^2\sin^2(\omega t) + \frac{J''}{2}\tilde{\theta}^2 - J''a\tilde{\theta}\sin(\omega t)$$

$$= J^* + \frac{a^2 J''}{4} - \frac{a^2 J''}{4}\cos(2\omega t)) + \frac{J''}{2}\tilde{\theta}^2 - J''a\tilde{\theta}\sin(\omega t)$$

Extremum Seeking Control

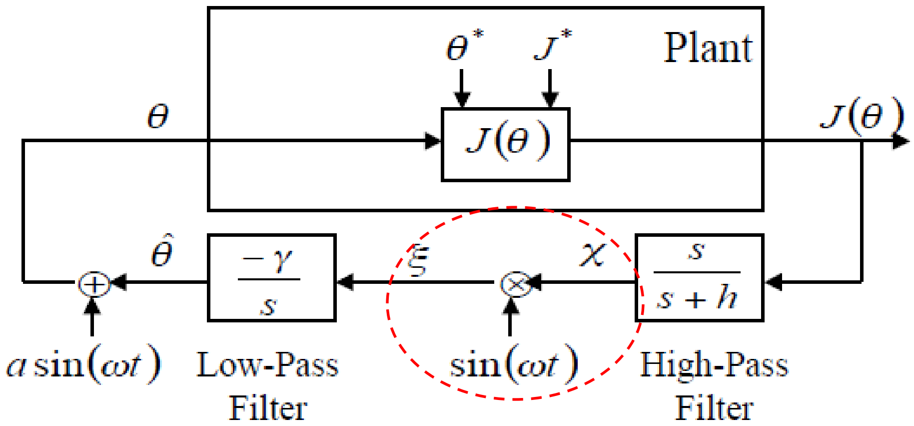

$$\chi(t) = -\frac{a^2 J''}{4}\cos(2\omega t)) + \frac{J''}{2}\tilde{\theta}^2 - J''a\tilde{\theta}\sin(\omega t)$$

$$\xi(t) = \chi(t)\sin(\omega t)$$

$$= -\frac{a^2 J''}{4}\sin(\omega t)\cos(2\omega t)) + \frac{J''}{2}\tilde{\theta}^2\sin(\omega t) - J''a\tilde{\theta}\sin^2(\omega t)$$

Extremum Seeking Control

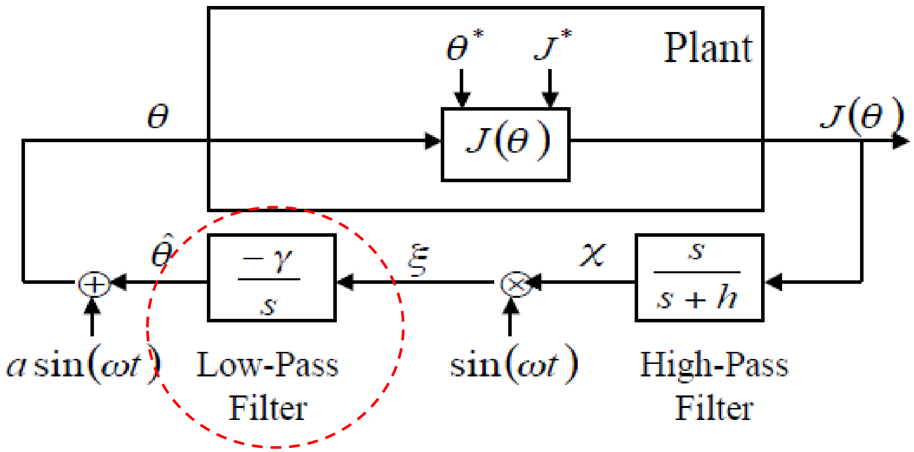

$$\xi(t) = -\frac{a^2 J''}{4}\sin(\omega t)\cos(2\omega t) + \frac{J''}{2}\tilde{\theta}^2 \sin(\omega t) - J''a\tilde{\theta}\sin^2(\omega t)$$

$$= -\frac{a^2 J''}{8}[\sin(3\omega t) - \sin(\omega t)] + \frac{J''}{2}\tilde{\theta}^2 \sin(\omega t) - \frac{J''a\tilde{\theta}}{2}[1 - \cos(2\omega t)]$$

$$= -\frac{J''a\tilde{\theta}}{2} + \frac{J''a\tilde{\theta}}{2}\cos(2\omega t) - \frac{a^2 J''}{8}[\sin(3\omega t) - \sin(\omega t)] + \frac{J''}{2}\tilde{\theta}^2 \sin(\omega t)$$

Extremum Seeking Control

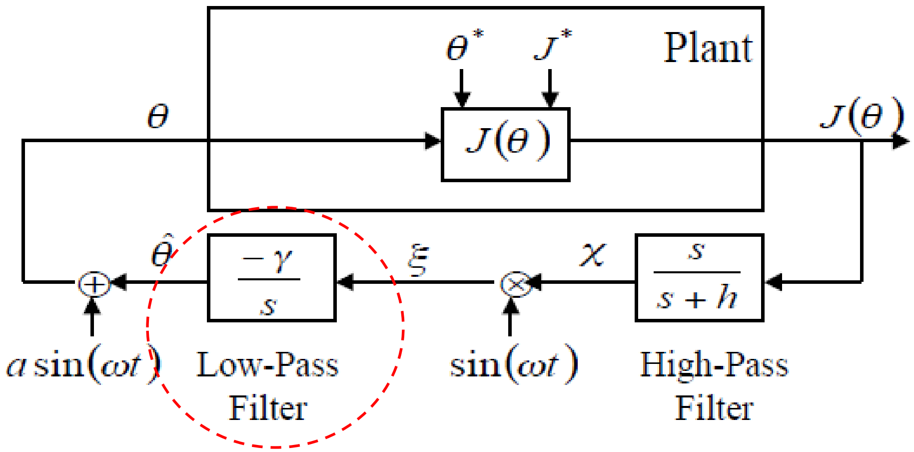

$$\hat{\theta}(t) = -\frac{\gamma}{s}\frac{J''a\tilde{\theta}(t)}{2} \rightarrow \dot{\hat{\theta}}(t) = -\frac{\gamma J''a\tilde{\theta}(t)}{2}$$

$$\xrightarrow{\tilde{\theta}=\theta^*-\hat{\theta}} \dot{\tilde{\theta}}(t) = -\frac{\gamma J''a\tilde{\theta}(t)}{2} \xrightarrow{\gamma J''a>0} \tilde{\theta}(t) \Rightarrow 0$$

$$\rightarrow \theta^* - \hat{\theta} \Rightarrow 0 \rightarrow \theta^* = \hat{\theta}$$